SPATIAL DNS OF THE FLOW TRANSITION OF A RECTANGULAR BUOYANT REACTING FREE-JET

Xi Jiang*
Department of Engineering, Queen Mary and Westfield College
University of London, London E1 4NS, UK
x.jiang@qmw.ac.uk

Kai H. Luo
Department of Engineering, Queen Mary and Westfield College
University of London, London E1 4NS, UK
k.h.luo@qmw.ac.uk

ABSTRACT

This paper describes a spatial direct numerical simulation of the flow transition of a buoyant diffusion flame established on a rectangular nozzle with an aspect ratio of 2:1. Without applying external perturbations, large vortical structures develop naturally in the flow field. At the downstream, the spatially developing reacting jet shows a tendency of transition to turbulence under the effects of combustion-induced buoyancy. Turbulent inertial range has been observed.

INTRODUCTION

As an efficient technique of passive flow control, noncircular jets are encountered in many engineering applications such as combustors, cooling of energy conversion devices, and exhaust of aerospace vehicles, as well as in environmental problems. In the last fifteen years, noncircular jets have been the topic of extensive research, both experimentally and numerically. The topic was recently reviewed by Gutmark and Grinstein (1999). In a broad range of practical applications, buoyancy due to density inhomogeneity under the influence of gravity plays a major role in the flow development. Buoyancy effects are especially important to low speed combustion applications. However, buoyancy effects have not been taken into consideration in the existing numerical studies of noncircular jets.

Free-jets in open-boundary domains with buoyancy effects are usually characterized by a turbulent, weakly buoyant far field and a strongly buoyant near field. The near-field dynamics, such as the formation and transport of vortices and laminar-to-turbulent flow transition, plays an important role in the spatial development of a jet flow. It has been understood that the flow instability of buoyant jets is fundamentally different from that of nonbuoyant jets. Buoyant jets and plumes display an intrinsic, absolutely unstable instability (Huerre and Monkewitz, 1990; Lingens *et al.*, 1996; Maxworthy, 1999), in which the evolution of vortices does not rely on the spatial amplification of external perturbation applied at the inflow boundary but on the gravitational effect due to the interaction between density gradients and gravity (Jiang and Luo, 2000). For the mean flow field, unlike the decay of streamwise velocity of nonbuoyant jets, the streamwise velocity of buoyant jets increases in the near field due to the buoyancy acceleration.

In light of the deficiency of numerical studies on noncircular jets with buoyancy effects, a direct numerical simulation (DNS) of a rectangular buoyant reacting jet with an aspect ratio of 2:1 on the nozzle plane is considered. The physical problem is a fuel jet issuing vertically into an ambient oxidant environment with a non-premixed flame established above the inlet plane. A fully three-dimensional (3D) simulation is performed. Since the primary focus of this study is on the combustion-induced buoyancy effects on the rectangular jet, not the details of the inner flame structure, a global, one-step reaction governed by temperature-dependent, finite-rate Arrhenius kinetics is used to represent the chemistry. This assumption has been made to avoid the prohibitively high costs of a fully 3D simulation with complex chemical kinetics.

*This work was funded by the UK Engineering and Physical Sciences Research Council under grant No. GR/L67271.

MATHEMATICAL FORMULATION

The governing equations used are the compressible time-dependent Navier-Stokes equations in non-dimensional form. Major reference quantities used in the normalization are: width of the fuel jet along the major axis of the rectangular nozzle, maximum velocity of the fuel jet at the nozzle, and ambient density, temperature and viscosity. The viscosity is chosen to be temperature-dependent according to $\mu = \mu_a(T/T_a)^{0.76}$. In the governing equations, $x-$direction is aligned with the minor axis of the rectangular nozzle, $y-$coordinate is along the major axis, and $z-$direction is assumed to be the streamwise (vertical) direction. The terms "major" and "minor" used here refer to the dimensions of the fuel jet on the inlet plane. The gravitational effect is expressed as buoyancy terms $(\rho_a - \rho)g/Fr$ and $(\rho_a - \rho)wg/Fr$ in the streamwise momentum equation and energy equation respectively, where Froude number is defined as $Fr = w_0^{*2}/(g_{ref}^* L_0^*)$ and g is the gravity imposed in the downwards vertical direction. The governing equations also include the perfect gas law for the mixture. A one-step global reaction with the non-dimensional reaction rate given by Luo (1999) is used. To isolate the effects of combustion-induced buoyancy, the fuel and oxidizer are assumed to be of equal molecular weight. The species are also assumed to be of equal viscosity.

A sixth-order accurate compact finite difference scheme (Lele, 1992) is used to evaluate the spatial derivatives in the governing equations in all the three directions. A third-order accurate fully-explicit compact-storage Runge-Kutta scheme is used to advance the equations in time. The specification of the boundary conditions is performed by using the general formulation of boundary conditions for DNS of Navier-Stokes equations by Poinsot and Lele (1992), which is based on the analysis of characteristics. The 3D computational domain is bounded by the inflow and outflow boundaries in the streamwise direction and the entrainment boundary in the cross-stream directions. Details of the boundary condition formulation can be found in Jiang and Luo (2000).

A "top-hat" profile is assumed for the streamwise velocity on the inlet plane, while the cross-streamwise velocity components are taken as zero. Due to the absolutely unstable nature of the flow, no perturbation was applied at the inflow boundary. The effect of buoyancy on the flow resolution sets a limit on the minimum value of Froude number that can be prescribed in a DNS of buoyant flows (Elghobashi *et al.*, 1999) under a certain number of grid points. The simulation has been performed with Froude number $Fr = 1.5$ and Reynolds number $Re = 1000$, bases on the inlet reference quantities. The ratio of specific heats, Prandtl and Schmidt numbers used in the simulation are chosen to be constants: $\gamma = 1.4$, $Pr = 1$ and $Sc = 1$. Parameters used for the chemical reaction are: Damköhler number $Da = 6$, Zeldovich number $Ze = 12$, flame temperature $T_f = 6$, and heat of combustion $Q_h = 1650$. The reason for the choice of these values is to mimic the behavior of a low heat release combustion under the computational restrictions of the DNS approach. The fuel temperature at the inlet is assumed to be 3, which was chosen to ensure autoignition of the mixture (Grinstein and Kailasanath, 1996). A computational domain of the size of $3\times6\times8$ with a grid system of $108 \times 216 \times 288$ nodes was used. The simulation was performed on the massively parallel computer Cray T3E-1200E in Manchester by using 72 processors. The results were tested as grid independent and time-step independent.

RESULTS AND DISCUSSION

The near field of the rectangular buoyant reacting jet is fully resolved in both space and time, which provides detailed information on the flow field that can be used to probe the flow physics. Due to the combustion-induced buoyancy, the reacting jet develops transitional behaviour under the moderate Reynolds number considered. The results are discussed in terms of instantaneous flow quantities, energy spectra, and time-averaged flow quantities. Focus has been given to the flow structures and transitional dynamics.

Buoyant jets and plumes display a periodic pulsation behavior known as "flickering" or "puffing" phenomenon associated with the formation and convection of buoyancy-induced large vortical structures in the near field (Cetegen *et al.*, 1998; Maxworthy, 1999; Jiang and Luo, 2000). Fig. 1 shows the temperature contours on the major axis plane of the rectangular reacting jet at two different times within one pulsation period. It is observed that large vortical structures evolve spatially in the flow field. Close to the inlet plane, the "necking" phenomenon can be observed, which is due to the buoyancy acceleration and flow entrainment. With the convection of the large vortical structures in the streamwise direction by the

mean flow, the flow exhibits a periodic behavior. The maximum flame temperature at a certain location of the flow field also changes with time due to the pulsation of the flow.

Figure 2 shows temperature contours on the minor axis plane. It is noticed that the reacting jet spreads rapidly in the minor axis direction at the downstream. Fig. 3 shows temperature contours on $z = 5.0$ plane at the downstream of the rectangular reacting jet. Due to the vortex deformation effects associated with the aspect ratio and corner features of the rectangular geometry (Gutmark and Grinstein, 1999), the reacting jet evolves spatially with complex 3D structures.

In the near field, a buoyant jet entrains its ambient fluids and the entrainment dominates the mixing. Fig. 4 shows the instantaneous entrainment characteristics of the reacting jet, which is the cross-streamwise velocities on the major axis plane at $z = 5.0$. The three different times shown in the figure correspond approximately to one pulsation period. Therefore the curves at $t = 22.0$ and $t = 24.0$ are almost overlapping. It is observed from this figure that the cross-streamwise velocity is very significant, which indicates a strong entrainment in the rectangular buoyant reacting jet.

Figure 5 shows history of the centerline streamwise velocities at different vertical locations of the rectangular buoyant reacting jet. The flow is fully developed approximately after $t = 12.0$. At the location of $z = 1.0$, the variation of the streamwise velocity is very regular due to the formation and convection of buoyancy-induced coherent structures associated with the "flickering" or "puffing" phenomenon. However, the flow becomes less coherent at the further downstream location of $z = 5.0$. The centerline streamwise velocity at this downstream location fluctuates more than that at $z = 1.0$ close to the inlet plane.

Figure 6 shows energy spectra determined from the history of the instantaneous centerline streamwise velocities at different vertical locations of the flow field by using Fourier analysis, which is presented in logarithmic scales (to the base 10) of the non-dimensional frequency (Strouhal number) and kinetic energy. The spectral analysis used velocity data taken over a time interval of six pulsation periods for the fully developed reacting jet after the initial stage of the simulation. It can be observed that the most energetic mode occurs at a low frequency, which is about $St = 0.5$. This frequency is the "puffing" or "flickering" frequency. It is also noticed that the flow becomes more energetic and higher frequency harmonics are developed in the flow field at the downstream.

The most important feature in Fig. 6 is the development of these high frequency harmonics associated with the breakdown of buoyancy-induced large scale structures at the downstream, which indicates the emergence of small-scale turbulence in the flow field. Flow transition to turbulence is the consequence of the breakdown of large scale vortical structures due to strong vortex interactions, especially the interactions between the streamwise vorticity and the cross-streamwise vorticity (Grinstein and DeVore, 1996). The quantitative trend of transition to turbulence can be measured by the Kolmogorov cascade theory, which states a power law correlation between the energy and frequency: $E(St) \sim St^{-5/3}$. Apparently the behavior of this rectangular reacting jet at the location of $z = 5.0$ follows the Kolmogorov cascade theory, indicating the occurrence of flow transition to turbulence at the downstream.

Vorticity is a transportable quantity and, once generated, it can be convected, diffused, augmented or terminated. The three components of vorticity are $\omega_x = \partial w/\partial y - \partial v/\partial z$, $\omega_y = \partial u/\partial z - \partial w/\partial x$, and $\omega_z = \partial v/\partial x - \partial u/\partial y$, respectively. The governing equation for vorticity transport in buoyant flows can be written in a vector form as

$$\frac{D\boldsymbol{\omega}}{Dt} = (\boldsymbol{\omega}\cdot\boldsymbol{\nabla})\mathbf{V} - \boldsymbol{\omega}(\boldsymbol{\nabla}\cdot\mathbf{V}) + \frac{1}{\rho^2}(\boldsymbol{\nabla}\rho\times\boldsymbol{\nabla}p) + \frac{1}{\rho^2}\frac{\rho_a}{Fr}(\boldsymbol{\nabla}\rho\times\mathbf{g}) + \boldsymbol{\nabla}\times(\frac{1}{\rho}\boldsymbol{\nabla}\cdot\boldsymbol{\tau})$$

The terms on the right hand side are the vortex stretching term, dilatation term, baroclinic torque, gravitational term, and viscous term, respectively. Among these five transport terms, it is known that the dilatation and viscous terms mainly attenuate flow vorticity (Givi, 1989). The relaminarization effect of chemical heat release on nonbuoyant jet flames such as observed by Grinstein and Kailasanath (1996) is mainly because of these two terms (Jiang and Luo, 2000). However, the importance of these two terms in the vorticity transport budget is insignificant for buoyant flows with moderately high Reynolds number and low Froude number (Jiang and Luo, 2000), such as the case investigated here.

The gravitational term due to the interac-

tion between density gradients and gravity is an important term in the vorticity generation. It is responsible for the absolute instability of the flow that can initiate vorticity (Jiang and Luo, 2000). This term does not contribute to the streamwise vorticity for the flow configuration studied. However, once the cross-streamwise vorticity ω_x and ω_y are generated, the significant vortex stretching $\omega_x\,\partial w/\partial x + \omega_y\,\partial w/\partial y + \omega_z\,\partial w/\partial z$ and baroclinic torque in the streamwise direction will subsequently lead to the development of streamwise vorticity.

Figure 7 shows history of the vorticity extrema in the computational domain of the rectangular reacting jet. The streamwise vorticity ω_z is initially zero, it develops with the vorticity in the cross-stream directions. When the flow reaches the periodic stage, the streamwise vorticity is about the same amplitude as the cross-streamwise vorticity ω_x in the minor axis direction. With the spatial development of the reacting jet, strong 3D vortex interactions occur at the downstream of the flow field due to the development of the significant streamwise vorticity. These interactions consequently lead to the breakdown of the large scale vortical structures, and flow transition occurs at the downstream of the reacting jet as shown in Fig. 6 by the energy spectrum. From Fig. 7, it also can be observed that the vorticity in the major axis direction ω_y is higher (in terms of absolute value) than that of the vorticity in the minor axis direction ω_x due to the aspect ratio effect of the rectangular geometry.

Time-averaged flow statistics are also of interests, which were obtained by averaging the flow quantities over six pulsation periods after the initial transients had been convected out of the computational domain. Figure 8 shows the time-averaged streamwise velocity contours at different vertical locations. For the mean flow field of noncircular jets, the most interesting discovery was the phenomenon of axis-switching (Gutmark and Grinstein, 1999). Jet spreading in the minor axis plane was observed to be much greater than that in the major axis plane due to the vortex deformation and self-induction processes associated with the aspect ratio and corner effects of noncircular jets (Grinstein and DeVore, 1996; Gutmark and Grinstein, 1999). From Fig. 8, it can be seen that the jet flow resembles its original rectangular shape close to the inlet plane, while it grows much faster in the minor axis direction further downstream due to the vortex self-induction effects. The results indicate the aspect ratio and corner features of the rectangular geometry. It is evident that this rectangular buoyant reacting jet has a tendency towards axis-switching similar to that observed for nonbuoyant jets.

SUMMARY

The near-field dynamics of buoyant jets, including flow instabilities, formation and interaction of the large scale vortical structures and transition to turbulence, is an area requiring a better understanding. This study provide a DNS attempt to the near-field dynamics of noncircular jet diffusion flames under the effects of buoyancy. The gravitational effect leads to the formation and development of large scale vortical structures in the flow field, and vortex breakdown and transition to turbulence occur at the downstream of the reacting jet due to strong 3D vortex interactions. This study highlights the importance of combustion-induced buoyancy on noncircular jet diffusion flames. The rectangular reacting jet shows a tendency towards axis-switching at the downstream.

REFERENCES

Cetegen, B. M., Dong, Y., and Soteriou, M. C., 1998, "Experiments on stability and oscillatory behavior of planar buoyant plumes", *Phys. Fluids*, Vol. 10, pp. 1658-1665.

Elghobashi, S., Zhong, R., and Boratav, O., 1999, "Effects of gravity on turbulent nonpremixed flames", *Phys. Fluids*, Vol. 11, pp. 3123-3135.

Givi, P., 1989, "Model-free simulations of turbulent reactive flows", *Prog. Energy Combust. Sci.*, Vol. 15, pp. 1-107.

Grinstein, F. F., and DeVore, C. R., 1996, "Dynamics of coherent structures and transition to turbulence in free square jets", *Phys. Fluids*, Vol. 8, pp. 1237-1251.

Grinstein, F. F., and Kailasanath, K., 1996, "Exothermicity and relaminarization effects in unsteady reactive square jets", *Combust. Sci. Technol.*, Vol. 114, pp. 291-312.

Gutmark, E. J., and Grinstein, F. F., 1999, "Flow control with noncircular jets", *Annu. Rev. Fluid Mech.*, Vol. 31, pp. 239-272.

Huerre, P., and Monkewitz, P. A., 1990, "Local and global instabilities in spatially developing flows", *Annu. Rev. Fluid Mech.*, Vol. 22, pp. 473-537.

Jiang, X., and Luo, K. H., 2000, "Spatial direct numerical simulation of the large vortical

structures in forced plumes", *Flow, Turbulence and Combustion*, Vol. 64, pp. 43-69.

Lele, S. K., 1992, "Compact finite difference schemes with spectral-like resolution", *J. Comput. Phys.*, Vol. 103, pp. 16-42.

Lingens, A., Reeker, M., and Schreiber, M., 1996, "Instability of buoyant diffusion flames", *Exp. Fluids*, Vol. 20, pp. 241-248.

Luo, K. H., 1999, "Combustion effects on turbulence in a partially premixed supersonic diffusion flame", *Combust. Flame*, Vol. 119, pp. 417-435.

Maxworthy, T., 1999, "The flickering candle: transition to a global oscillation in a thermal plume", *J. Fluid Mech.*, Vol. 390, pp. 297-323.

Poinsot, T. J., and Lele, S. K., 1992, "Boundary conditions for direct simulations of compressible viscous flows", *J. Comput. Phys.*, Vol. 101, pp. 104-129.

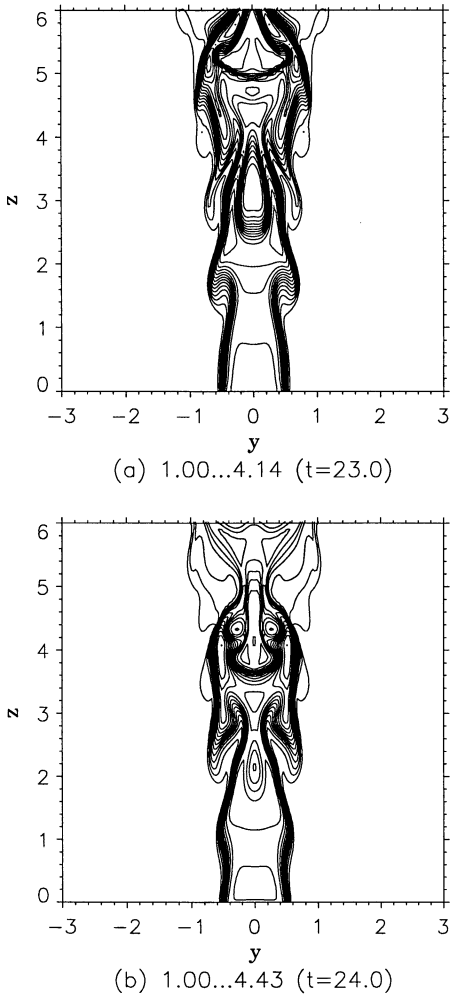

Figure 1: Temperature contours on the major axis plane of the rectangular buoyant reacting jet (15 contours between the minimum and maximum as indicated).

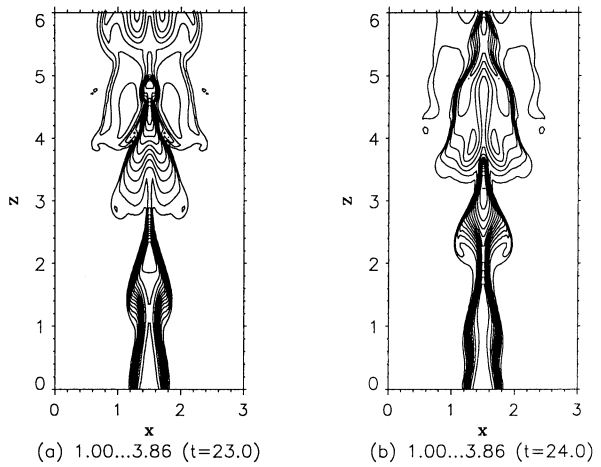

Figure 2: Temperature contours on the minor axis plane of the rectangular buoyant reacting jet (15 contours between the minimum and maximum as indicated).

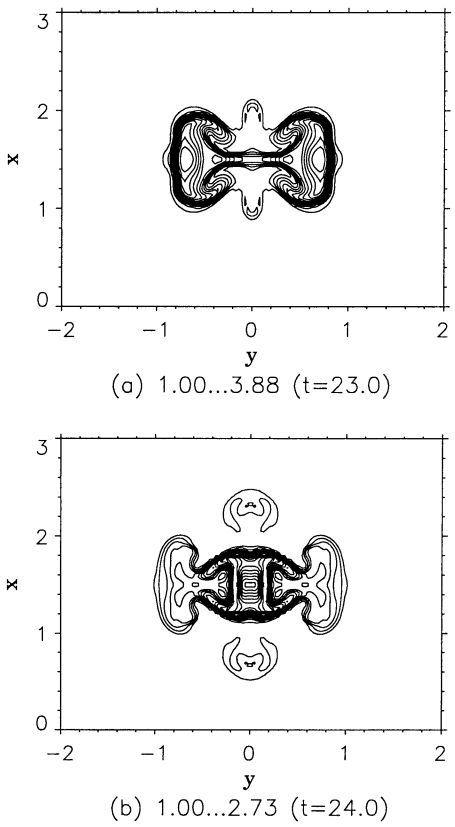

Figure 3: Temperature contours on $z = 5.0$ plane of the rectangular buoyant reacting jet (15 contours between the minimum and maximum as indicated).

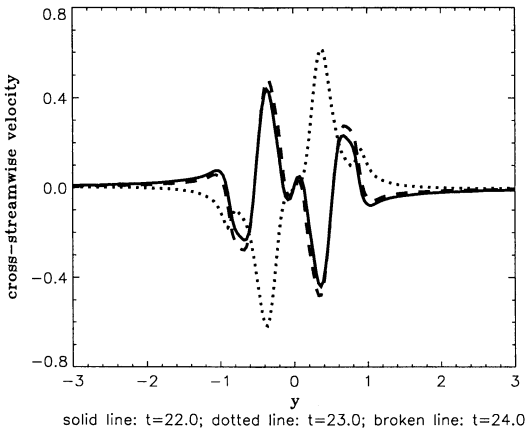

Figure 4: Instantaneous cross-streamwise velocities on the major axis plane at $z = 5.0$ of the rectangular buoyant reacting jet.

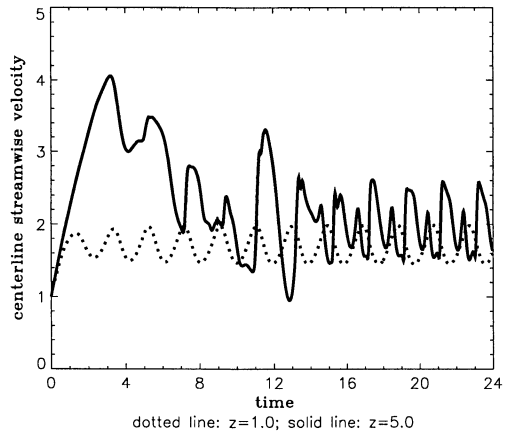

Figure 5: History of the centerline streamwise velocities at different vertical locations of the rectangular buoyant reacting jet.

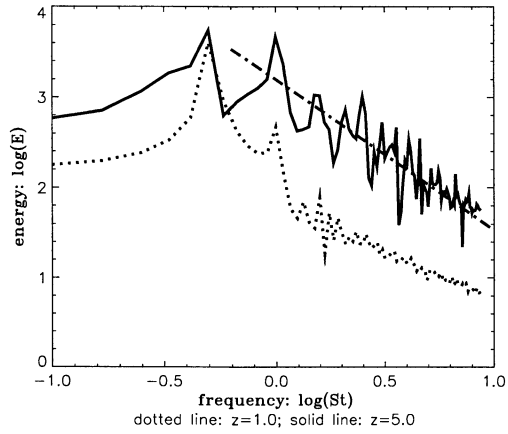

Figure 6: Energy spectra of the centerline streamwise velocities at different vertical locations of the rectangular buoyant reacting jet (chained line: Kolmogorov cascade theory $E(St) \sim St^{-5/3}$).

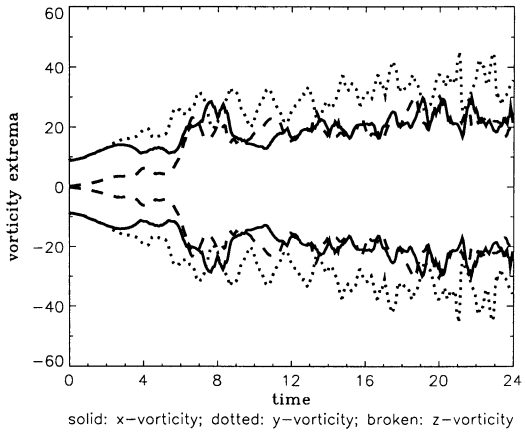

Figure 7: History of the vorticity extrema of the rectangular buoyant reacting jet.

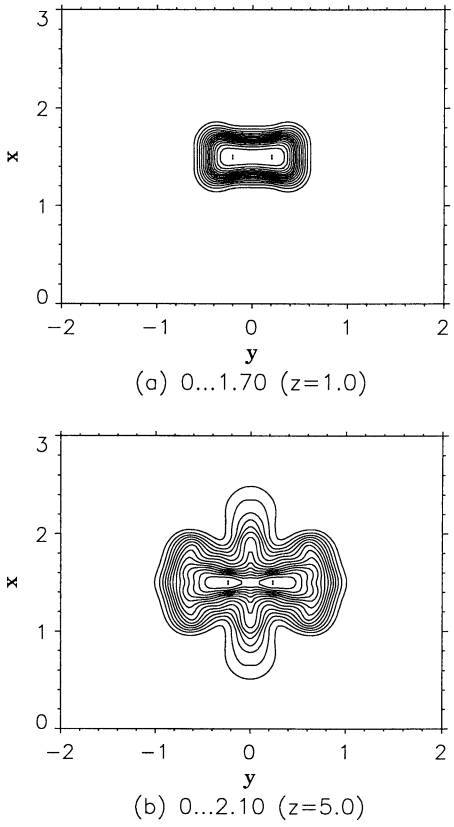

Figure 8: Time-averaged streamwise velocity contours at different vertical locations of the rectangular buoyant reacting jet (15 contours between the minimum and maximum as indicated).